Marine Pollution Bulletin 187 (2023) 114533

Contents lists available at ScienceDirect

Marine Pollution Bulletin

journal homepage: www.elsevier.com/locate/marpolbul

Influence of waves on the three-dimensional distribution of plastic in the ocean

Raphaël Bajon [*,1], Thierry Huck, Nicolas Grima, Christophe Maes, Bruno Blanke, Camille Richon, Xavier Couvelard

Laboratoire d'Océanographie Physique et Spatiale (UMR 6523 LOPS), Univ. Brest, CNRS, Ifremer, IRD, IUEM, Technopole Brest-Iroise, Plouzané 29280, France

ARTICLE INFO

Keywords:
Microplastics
Marine debris
Plastic discharge
Ocean-wave coupling
Stokes drift
Three-dimensional circulation

ABSTRACT

The world's oceans are facing plastic pollution, 80 % of which of terrestrial origin flowing from the mismanaged waste of coastal populations and from river discharge. To study the fate of this pollution, the three-dimensional trajectories of neutral plastic particles continuously released for 24 years according to realistic source scenarios are computed using currents from a global ocean-wave coupled model at $\frac{1}{4}^{\circ}$ resolution and from a reference ocean-only model. These Lagrangian simulations show that neutral particles accumulate at the surface in the subtropical convergence zones from where they penetrate to about 250 m depth and strongly disperse over 40° of latitude. About 5.3 % of the particles remain at the surface with the wave-coupled model currents, whereas only 2 % for the uncoupled model, with some modulation in the location of the convergence zones. Increased surface retention results from upward vertical velocities induced by widespread divergence of waves-induced Stokes transport in the surface layers.

1. Introduction

World plastic production is currently close to 400 million tons per year (Plastics Europe, 2019). This figure has been increasing exponentially since the 1950s (Geyer et al., 2017; Lau et al., 2020). The array of countries and differing degrees of technological advances in recycling and people's awareness means that a significant part of this global plastic production will enter the oceans sooner or later. Even a country with ample environmental awareness and optimal technologies will not be able to zero out its discharge of plastic into nature – called "Mismanaged Plastic Waste" (MPW) in the literature – because plastic is still extensively used in many fields and the entry ways remain excessive. Moreover, its danger for the ecosystem is well known (Wright et al., 2013) and demonstrated through numerous studies, and the presence of microplastics (defined as plastics with characteristic dimensions smaller than 5 mm) in the digestive system of zooplankton leads to many uncertainties (Law, 2017).

The weight of plastic entering the oceans has been estimated between 4.8 and 12.7 million tons per year by Jambeck et al. (2015), i.e., 1.3 to 3.3 % of annual production (Geyer et al., 2017). About 80 % of plastics in the oceans come from land (GESAMP, 2015) compared to the 20 % from marine sources (Jambeck et al., 2015), such as commercial fishing, shipping and cruises (Lebreton et al., 2012). Land-based plastic entering the marine environment finds its way via rivers and watersheds (Lebreton et al., 2017) (1.15 to 2.41 million tons via rivers according to Lebreton et al. (2017)) but also via coastal populations (3.1 to 8.2, 4.8 to 12.7 million tons according to Jambeck et al. (2015); Lebreton and Andrady (2019) respectively). Regions with high-population densities and poorly developed plastic recycling and waste treatment facilities are important coastal sources of plastic waste to the ocean (Lebreton and Andrady, 2019). Estimates of the total amount of plastic entering the oceans each year vary according to the assumptions considered (from a few hundred thousand to several million tons). (Jambeck et al., 2015; Lebreton et al., 2017; Schmidt et al., 2017; Lebreton and Andrady, 2019; Borrelle et al., 2020). Nevertheless, the amount of plastics on the surface of the oceans is considerably less than the estimated inflow (Cózar et al., 2014; Eriksen et al., 2014; van Sebille et al., 2015). Plastic at the sea surface is found concentrated in the subtropical gyres (Cózar et al., 2014; Isobe et al., 2021) due to the convergence of wind-driven Ekman currents (Kubota, 1994; Martinez et al., 2009; Onink et al., 2019). In

* Corresponding author.
E-mail addresses: raphael.bajon@ifremer.fr (R. Bajon), thierry.huck@univ-brest.fr (T. Huck), nicolas.grima@univ-brest.fr (N. Grima), christophe.maes@ird.fr (C. Maes), blanke@univ-brest.fr (B. Blanke), camille.richon@univ-brest.fr (C. Richon), xaviercouvelard@gmail.com (X. Couvelard).
[1] https://raphaelbajon.github.io, https://www.linkedin.com/in/raphael-bajon.

https://doi.org/10.1016/j.marpolbul.2022.114533
Received 2 November 2022; Received in revised form 22 December 2022; Accepted 24 December 2022
Available online 5 January 2023

fact, plastic has been found throughout the water column (Kooi et al., 2017; Pabortsava and Lampitt, 2020; Tekman et al., 2020; Vega-Moreno et al., 2021; Ross et al., 2021; Zhao et al., 2022) and the "missing" plastic may be within the water column and in marine sediments (Woodall et al., 2014; Mountford and Morales Maqueda, 2019; van Sebille et al., 2020). The behaviour of plastic pathways in the oceans depends on the property of the component, such as its extrinsic density. Yet, due to the wide variety of plastic densities, some of which are close to that of seawater, plastic at sea is therefore a combination of floating, neutral and sinking particles. Various studies already discuss their proportion in the oceans (Geyer et al., 2017; Andrady, 2011; Mountford and Morales Maqueda, 2019). In addition to the wide variety of plastic densities, particles are also subject to oceanic currents, waves, turbulence and vertical mixing on entering the ocean (Kukulka et al., 2012; Reisser et al., 2015; Onink et al., 2022), as they can dictate and alter their trajectory. Moreover, plastic particles at sea are exposed to degradation and fragmentation, due to biological, chemical and physical processes such as UV exposure, mechanical stirring, and biofouling, which all alter their buoyancy (van Sebille et al., 2020). Hence, all the complex processes affecting plastic transport are poorly quantified (Lobelle et al., 2021).

Given the scarcity of available data and observations on marine litter and plastic pollution (Galgani et al., 2021), even less frequent in the water column, numerical simulations could provide answers to some questions and "fill a gap" as proposed by van Sebille et al. (2020). Numerical models and Lagrangian tracking are a well-tested way to study water mass and particle transport (see Blanke et al., 2002; Speich et al., 2006, 2007, for examples of global ocean water mass studies). The majority of previous studies on microplastic transport using numerical simulations have focused on the surface (i.e., in a 2D framework Maximenko et al., 2012; Lebreton et al., 2012; van Sebille et al., 2012; Maes et al., 2018; Dobler et al., 2019; Chenillat et al., 2021). However, the movement of plastic in the sea is three-dimensional, particularly as it is affected by the physical and biological processes mentioned above which alter its trajectory (Jalón-Rojas et al., 2019; van Gennip et al., 2019; Lobelle et al., 2021). Furthermore, plastic pollution must be considered a global problem (Maes et al., 2019) and not restricted to an individual region (Blackwatters et al., 2020).

Surface waves have been shown to have a critical influence on the fate of particles floating at the ocean surface (Dobler et al., 2019; Onink et al., 2019) through their net transport and Stokes drift, but the three-dimensional coupling of surface waves with ocean circulation is far more complex, involving primarily the influence of wave height on the vertical mixing of heat and momentum. Global coupled wave-ocean models have been developed over the recent years (Breivik et al., 2015; Couvelard et al., 2020) and now allow investigating the influence of wave dynamics on the 3D dispersion of "plastic" particles at sea (Huck et al., 2022).

The contribution of waves will be studied with a coupled model taking into account the wave dynamics, including Stokes drift, in a consistent manner, and comparisons will be made with the currents from the same ocean model but uncoupled. Plastic release and dispersion at sea is a global problem, with intricate connections between remote regions (Chassignet et al., 2021; Chenillat et al., 2021). Unfortunately, global ocean-wave coupled models are still in their infancy and run at lower horizontal resolution (1/4°) than state-of-the-art ocean models (1/12° and higher). This study is thus a first step in assessing the influence of wave dynamics on neutral plastic distribution in the ocean. Moreover, it aims to provide better estimates of the distribution of plastics following a realistic release scenario, consequent to recent estimates of coastal population and river input.

The paper is organized as follows. Section 2 describes the numerical Lagrangian experiments. Section 3 presents the results in terms of the final horizontal and vertical particle distributions, before investigating the reasons for the discrepancies between the coupled and uncoupled approaches through the examination of their vertical velocities. Conclusions and their discussion follow in Section 4.

2. Methods

2.1. The Ariane Lagrangian tool

We used the Ariane Lagrangian application with a setup similar to that of Huck et al. (2022), now with changes in the model used and a more advanced scenario of plastic release into the ocean. The model and simulations are briefly described below.

The Ariane Lagrangian software (Blanke and Raynaud, 1997) allows the exact computation of 3D trajectories of numerical particles in stationary and non-divergent transport fields, defined on a C-grid (Arakawa and Lamb, 1977). Two modes are available in this application ('qualitative' or 'quantitative'). In this study, we used the 'qualitative' mode that allows to follow the trajectories of numerical particles released at any position and time. Here, particles were released continuously in time along the coastline according to plastic discharge scenarios. The application sequentially reads archived velocity field values of a global ocean circulation model, advects the particles and computes their trajectories.

The Ariane application uses the velocity discretization properties on a C-grid and of volume conservation to analytically compute the particle trajectories. Between two temporal updates of the velocity field, the 3D velocity components are assumed to be stationary, so that the algorithm computes the actual trajectories by exact calculation of the three-dimensional streamlines (Blanke and Raynaud, 1997). Under this assumption of stationarity, these streamlines effectively represent the trajectories of particles advected by the given velocity field. Thus, considering the exact conservation of mass and a transport at the land/sea interface equal to zero, it is impossible for a particle to reach a land grid cell or to be trapped at the coast.

The method allows storage and access to the complete history of particle trajectories and, in particular, the connectivity between different regions of an ocean model. Because the application works with archived model outputs, it is also possible to advect numerical particles backward in time and assess the origins of the particles.

2.2. Ocean currents

The currents were taken from five-day average outputs of global ocean simulations using the Nucleus for European Modeling of the Ocean model (NEMO version 3.6, Madec, 2012) run at 1/4° horizontal resolution (Couvelard et al., 2020). On the vertical, 75 "z" levels were used with thicknesses increasing from 1 m close to the surface to 200 m at the bottom. A reference simulation was first performed using only NEMO following Barnier et al. (2006), which will be referred to as NEMOREF. Then the NEMO model was coupled with the WaveWatch III (WW3) wave model WAVEWATCH III® Development Group, 2016), using a 1/2° global configuration. Several coupled simulations were performed by progressively implementing all coupling terms. The coupled simulations were first performed over two years, 2013 being the spin-up and 2014 was analyzed in Couvelard et al. (2020). The fully coupled simulation was continued until the end of 2017, so that four full years were used for the present Lagrangian experiments, from 2014 to 2017 - this will be referred to as NEMOWAVE.

The NEMOREF and NEMOWAVE simulations share the same grid and output frequency. These outputs are used to compute the Lagrangian particle trajectories, but because it takes several years or decades for particles released at the coast to converge to the center of the subtropical convergence zones (Maximenko et al., 2012), we cycle through these four available years (2014–2017) six times to obtain 24-year-long simulations.

2.3. Plastic discharges

The realistic scenario of land-based plastic release in this paper is derived from the combination of two sources, coastal population and rivers (Fig. 1), which account for >80 % of plastics at sea (Jambeck et al., 2015). Indeed, plastics in the oceans come mainly from two sources: waste from coastal populations (40 % of the world's population lives within 100 km of the coastline) and rivers that can drain large catchments of waste into the oceans (Jambeck et al., 2015; van Sebille et al., 2020). These two categories have been estimated in the literature in a few studies (Jambeck et al., 2015; Schmidt et al., 2017; Lebreton et al., 2017; Lebreton and Andrady, 2019; Weiss et al., 2021) differing in amplitudes, though two of them show some consistency: Lebreton et al. (2017); Lebreton and Andrady (2019). Chassignet et al. (2021) have already implemented and discussed such a hybrid release scenario for Lagrangian experiments in a 2D surface framework. We follow here the same procedure in 3D, taking into account the estimates to date of plastic at sea from land. For coastal population discharge, we use the estimate by Lebreton and Andrady (2019): an annual value of mismanaged waste by populations is given per square kilometer of land (Mt y^{-1}) for the year 2015. From this data, only points within 50 km of the coastline were taken to estimate a coastal population MPW. One fourth of the present MPW is supposed to enter the ocean and accounts for the 5.1 Mt estimated in the literature (Lebreton and Andrady, 2019; Chassignet et al., 2021) (Fig. 1). For plastic inputs from rivers, which represent 1.4 Mt of plastic per year, we follow Lebreton et al. (2017) monthly estimates provided for 40,760 watersheds worldwide to represent their seasonal cycle properly, which may interact nonlinearly with the seasonal variations of ocean circulation, especially in Asian regions affected by monsoons. (van der Mheen et al., 2019; Pattiaratchi et al., 2022).

Annual MPW estimates from the coastal population (in Mt y^{-1}) were released at a monthly frequency in line with the monthly inputs from rivers in the simulations and better reflect the continuity of discharges. These quantities of plastic released into the ocean, initially expressed in millions of tons in these two scenarios, were then converted into equivalent numbers of particles per month to be tracked by the Lagrangian software (i.e., initialized to have a discharge every month in the 24-year simulations). The MPW given in tons and its equivalent number of numerical particles are presented in Fig. 1. We conducted some weighting on the initial plastic values to reach eight million particles at the end of the 24-year simulation for both scenarios and to save computational time. >95 % of the releases by weight for each scenario (waste from coastal populations or from rivers) could thus be processed. The two plastic release scenarios, population and rivers, were then summed to account for the fully realistic release that will be analyzed hereafter (Fig. 1). Particles are released continuously throughout the 24-year simulation with no evolution of fluxes through time. About 350,000 particles are released annually for both coastal population and river discharge scenarios, accounting for 5.1 and 1.4 Mt of annual plastic release from land to sea, respectively. In total, >16 million particles were tracked, all discharge scenarios combined. For more details on each scenario and their use, please refer to the python codes and data transmitted via Github (and to Fig. 1).

Knowing the amount of plastic in millions of tons per year entering the oceans for each scenario, the final results are given in terms of plastic concentration (g m^{-3}), which is more meaningful than a number of particles and independent of the numerical implementation of the Lagrangian experiments.

In summary, NEMOREF is the reference global ocean circulation simulation (NEMO ORCA 1/4°), whereas NEMOWAVE is the coupled wave-ocean simulation (NEMO ORCA 1/4° <=> WW3 1/2°). The NEMO ocean model uses a C-grid discretization with 1440 × 1050 grid points in longitude and latitude respectively, and 75 vertical levels. In

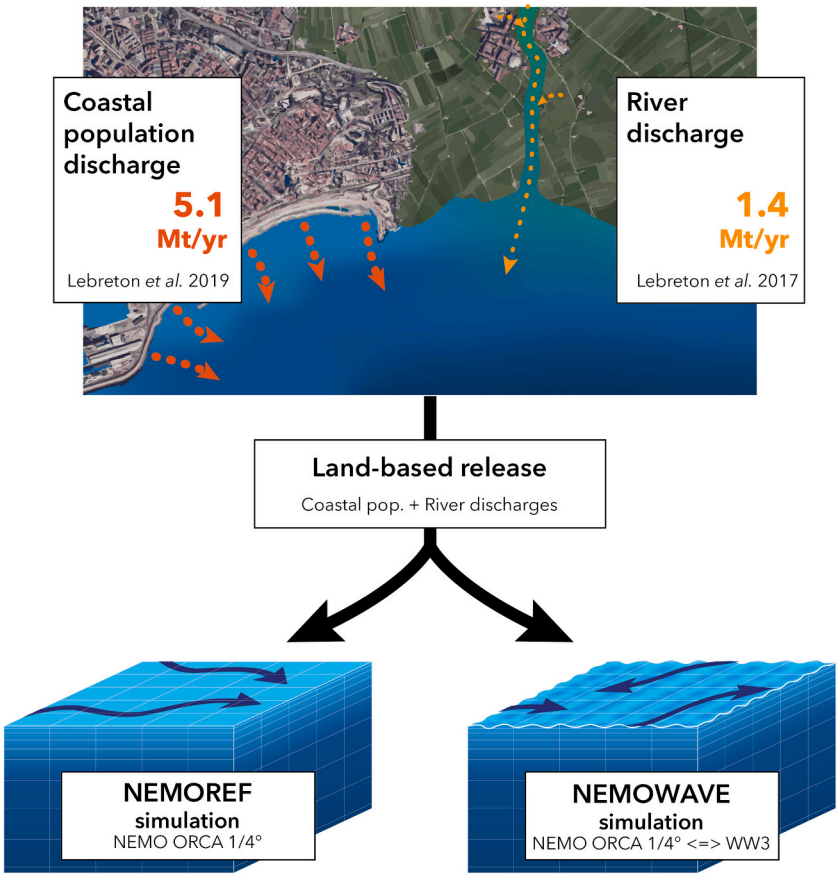

Fig. 1. Schematic summary of the particle release scenarios implemented in the Lagrangian experiments using the 3D velocity fields of the two simulations, NEMOREF and NEMOWAVE, with the corresponding amount of waste released annually into the ocean. NEMOREF is the reference global ocean circulation simulation (NEMO ORCA 1/4°), whereas NEMOWAVE is the coupled wave-ocean simulation (NEMO ORCA 1/4° <=> WW3 1/2°). The NEMO ocean model uses a C-grid discretization with 1440 × 1050 grid points in longitude and latitude respectively, and 75 vertical levels. In the Lagrangian simulations, 695,040 particles are released each year accounting for the land-based release (5.1 + 1.4 = 6.5 Mt yr^{-1}). At the end of the 24-year simulation, a total of 16,680,960 plastic particles are released. We compare hereafter the final concentration of plastics inferred from the number of particles of the Lagrangian simulations with NEMOREF and NEMOWAVE currents on the full land-based release.

the Lagrangian simulations, 695,040 particles are released each year accounting for land-based release ($5.1 + 1.4 = 6.5$ Mt yr^{-1}). At the end of the 24-year simulation, a total of 16,680,960 plastic particles are released. We compare hereafter the final concentration of plastics inferred from the number of particles of the Lagrangian simulations with NEMOREF and NEMOWAVE currents on the full land-based release. A concentration reference would be a uniform three-dimensional distribution of plastic, i.e. $\frac{\text{plastic mass:6.5 Mt yr}^{-1}\cdot\text{24 yr=156 Mt}}{\text{ocean volume:1,332 million km}^3} = 1.2{\cdot}10^{-4}$ g m^{-3}.

3. Results

3.1. Horizontal distribution

At the end of simulations, plastic particles are dispersed across all oceanic basins and the vertically integrated plastic concentration is not fundamentally different between the coupled (Fig. 2a) and uncoupled experiments (Fig. 2c). The zones of high concentration summed over depth are located in the center of each ocean basin, with a predominance of the Indian Ocean and North Pacific for the highest budget of plastic. Indeed, their proximity to areas of release makes them more likely to accumulate plastics. Conversely, the South Pacific Ocean does not

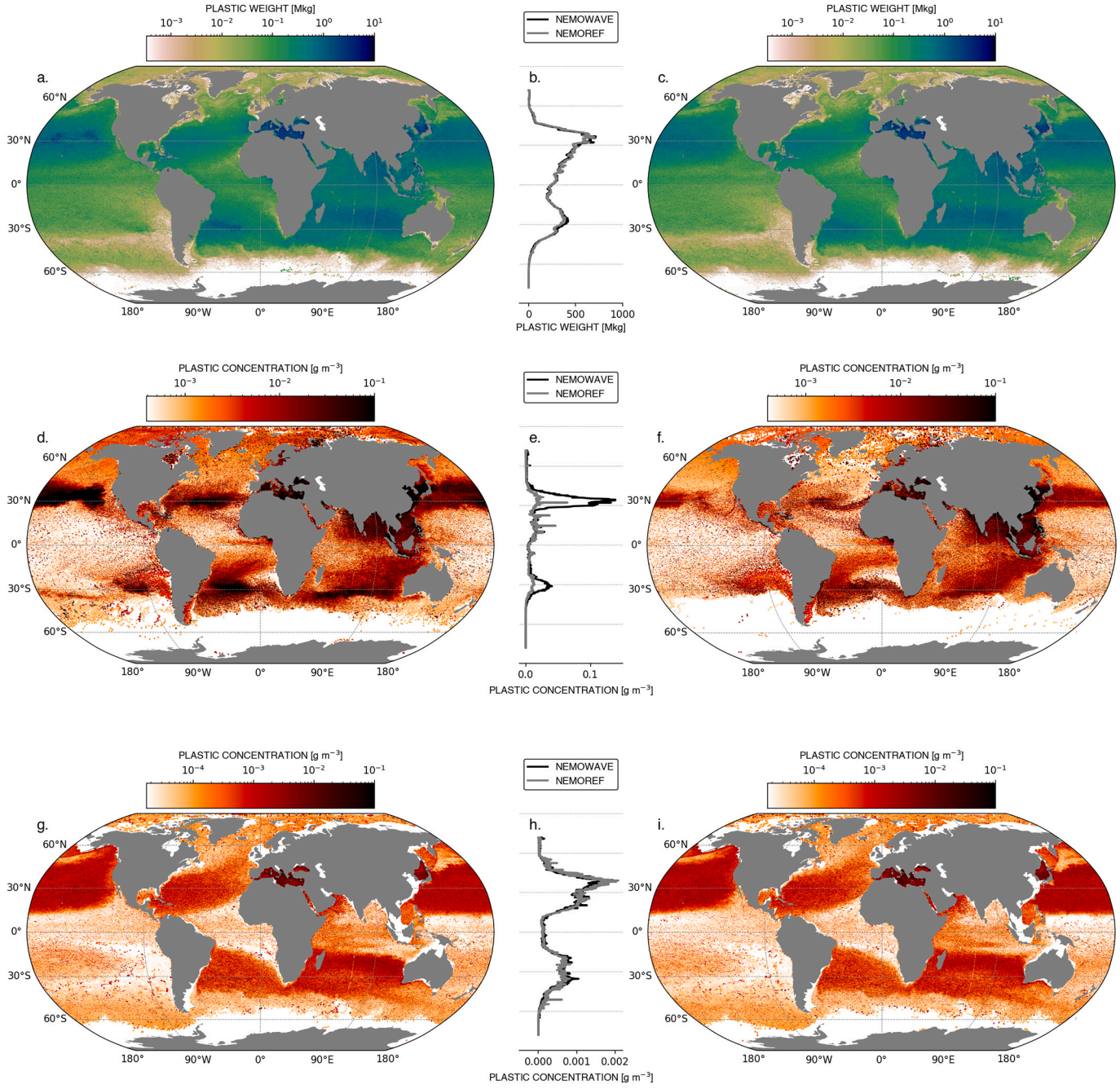

Fig. 2. Horizontal distribution of plastics at different depths, averaged over the last year (24) of the Lagrangian simulations with the (a,d,g) NEMOWAVE and (c,f,i) NEMOREF currents. (a,c) Plastic weight summed over depth in million kilograms, and integrated zonally as a function of latitude (b). Plastic concentration at the surface level (depth 0.5 m) (d,f) and at 240 m (g,i), and averaged zonally as a function of latitude (respectively e,h). The different color bars are expressed in logarithmic scale of (a) plastic waste (in M kg) or (c,e) concentrations (in g m^{-3}) and their ranges differ according to the case considered.

concentrate as many particles, as the amount of neighbouring discharge is notably smaller, according to Lebreton et al. (2017); Lebreton and Andrady (2019), than other regions. However, plastics remain at its surface for both experiments (Fig. 2d, f) with few particles. Nearly closed basins such as the Mediterranean Sea are highly concentrated in particles, due to the high population density in coastal areas.

The main differences between the coupled (NEMOWAVE) and uncoupled (NEMOREF) results are seen at the surface for the horizontal dispersion of plastic particles. Globally, plastics are widely dispersed over the surface layer for the coupled experiment with a higher concentration of particles for northern high latitudes, with 0.15 g m^{-1} at 30°N compared to 0.04 g m^{-1} at 30°S: ocean basins appear to be more affected in their surface layer by plastic pollution with the NEMOWAVE coupled simulation. In contrast, plastic concentrations are localized between 45°N and 35°S in the NEMOREF and do not reach latitudes above 60°N (Fig. 2f). Considering the different ocean basins distinctly, NEMOWAVE concentrates more plastic particles in the different subtropical gyres than NEMOREF (maximum concentrations around 0.15 g m^{-1} in NEMOWAVE vs. 0.07 g m^{-1} in NEMOREF for the same latitudes at 30°N). The surface level of the NEMOWAVE coupled experiment (Fig. 2a) shows a major contribution of the North Pacific Subtropical Gyre (NPSG) around [150°W, 30°N], in the concentration of microplastics (Table 1). The concentrations are very high in the gyre and extends to the East Asian coasts where its main plastic sources are located, leading to trapping large quantities of plastic in the area. In contrast, the uncoupled simulation leads to fewer plastic in the same NPSG and the zone of high concentration within this gyre extends over a smaller area (Fig. 2f). The South Pacific subtropical gyre (SPSG) is more homogeneous in plastic particles down to 35°S for NEMOREF whereas pathways are already evidenced at the surface, with contrasting high and low concentrations within this zone, for the NEMOWAVE coupled experiment.

We observe high plastic concentrations in the Atlantic Ocean for both NEMOREF and NEMOWAVE simulations, but the coupled experiment highlights different geometries of the two subtropical gyres within the Atlantic basin (Fig. 2f and Fig. 2d). The gyre in the North Altantic extends from Morocco to eastern America for the coupled experiment NEMOWAVE (Fig. 2d) whereas the zone of high concentration is located in the center of the basin for NEMOREF, and the Canary Current near the Mediterranean Sea is highly visible (Fig. 2f). Plastic concentrations in the gyres are not only locally more uniform meridionally for the coupled experiment, but also more homogeneous and higher, shifting north or south (Fig. 2d) from the theoretical 30° North/South positions of the gyres. The South Atlantic Ocean also shows different behaviour in the two simulations. The Agulhas Current flows down South Africa, linking the Indian Ocean basin and the South Atlantic for both experiments, but plastics cover a larger part of the South Atlantic basin in the NEMOWAVE experiment.

Plastic concentrations in the Indian Ocean are high, from 40°S to its land boundaries, with the greatest concentrations at the surface close to land emission regions (India and islands such as Sri Lanka and Sumatra) and within the large gyre from Africa to Australia (Fig. 2d) centered at 34°S with 0.04 g m^{-1}. This same region is not as concentrated in particles for the uncoupled experiment (Fig. 2f), near 0.02 g m^{-1}. Indeed, concentrations in the basin are more homogeneous, with reduced plastic concentration for the uncoupled simulation.

Going deeper into the water column highlights vast regions of dispersion for plastic particles entering the different ocean basins, for both the uncoupled (Fig. 2i) and coupled (Fig. 2g) experiments. Large regions of homogeneous concentration are represented in the different ocean basins except the South Pacific. The largest is located below the NPSG, strongly concentrated in particles compared to the other basins. The main characteristics of these extensions are the spread of high plastic concentrations over about 40° of latitude. The location of the maximum concentration differs between the coupled and uncoupled experiments while both are located in the Pacific Ocean. However, for the surface layer, the maximum concentration remains close to the East Asian emission region. The similarities are more interesting to show at this depth because the Stokes drift, provoked by waves, is a physical phenomenon acting mainly on the surface layers by definition. It is also important to note the concentrated region of the Mediterranean Sea for a depth level around 200 m. At this depth, this almost closed basin is the most concentrated in plastic. At the surface, plastic does not pass through the Antarctic Circumpolar Current (Fig. 2d,f), but at 240 m water depth it extends further south (Fig. 2g,i).

3.2. Vertical distribution

The zonally averaged concentration of microplastics is presented in Fig. 3 for the different ocean basins for the coupled experiment. In line with the previous observations, concentrations are very low at depths >1000 m, and very high at shallower depths, particularly for the first meters below the surface. Plastic concentrations are thus mainly located in the thermocline (Huang, 2015) and surface layers, in all oceans, and are similar to previous high-resolution results (Huck et al., 2022). Plastics remain in the surface layers above 500 m in the tropics, and enter deeper waters at high latitudes, easily reaching 1000 m near 40°S/N (Fig. 3c,d,e,f,i,j,k,l), below the subtropical gyres. Moreover, particles penetrate deeper in the northern hemisphere due to the formation of North Atlantic Deep Water south of Greenland at 45–50°N. An important conduit from the North Pacific also goes down to a depth of 2500 m at 30°N. Indeed, not only do particles penetrate the deep layers at these latitudes, but microplastic concentrations are higher around these latitudes (30°N/S). Hence, the partitioning of plastics with depth is heterogeneous depending on the ocean basin and latitude considered. The dispersion over >40° latitude previously seen in Fig. 2g and i is visible for the different basins just below the sea surface in both experiments (Fig. 3).

The Indian Ocean is the most concentrated basin with a mean concentration of $8.1{\cdot}10^{-4}$ g m^{-3}. In the Pacific Ocean, the NPSG traps particles at its surface, leading to a mean concentration of $4.6{\cdot}10^{-4}$ g m^{-3} and a maximum concentration of plastic reaching 0.25 g m^{-3}, which makes it the second largest reservoir of plastic in the ocean, after the Indian Ocean. The Atlantic Ocean appears to be the least polluted with plastic with a zonal mean concentration of $3.7{\cdot}10^{-4}$ g m^{-3} and a maximum plastic concentration of an order of magnitude lower than those in the other basins. Currents and the origin of particles have a major impact on the distribution of plastic concentration.

Plastic concentration at the surface is highly disparate between the uncoupled NEMOREF and coupled NEMOWAVE experiments, as already highlighted by the horizontal distributions (Fig. 2d,f)). At the surface, >0.1 g m^{-3} of plastic is found with the coupled model with waves, by

Table 1
Average distribution of plastic by depth for the last year of simulation (year 24), for the reference ocean experiment NEMOREF and the coupled experiment NEMOWAVE. Percentages indicate the fraction of the total quantity of plastic, i.e., the 156 Mt released in the land scenario over the 24-year period. Layer weights in million tons of plastic [Mt] are given in the Mt columns. Layer weights are ranked according to the following scale [− −, −, ±, +, ++] with − − and ++ characterizing the smallest and largest weight of plastic, respectively. Changes (negative/positive) from the uncoupled to the coupled simulation are categorized as small changes (~↓/~↑, <1 %) and high changes (⇓/⇑, >1 %).

Depth range [m]	Simulation				Changes
	NEMOREF		NEMOWAVE		
	fraction	Mt	fraction	Mt	
0 > z > − 1	2.44 %	3.8	5.24 %	8.2	− ⇑
- 1 > z > − 10	7.34 %	11.4	7.40 %	11.5	± ~ ↑
- 10 > z > − 100	32.60 %	50.9	31.68 %	49.4	+ ~↓
- 100 > z > − 1000	56.22 %	87.7	53.84 %	84.0	++ ⇓
- 1000 > z	1.40 %	2.2	1.84 %	2.9	− − ~↑

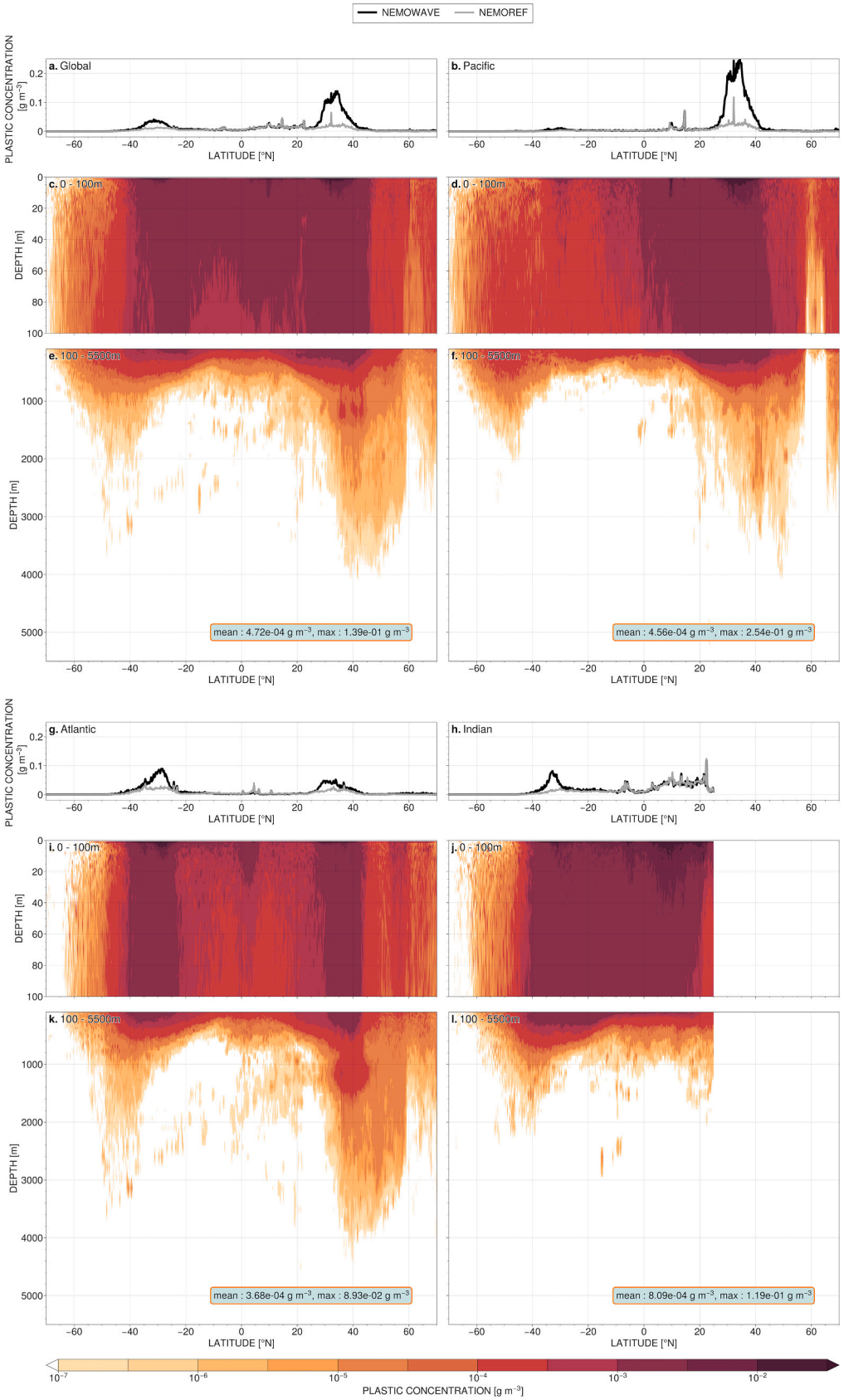

Fig. 3. Zonal mean plastic concentrations (g m^{-3}) as a function of latitude and depth, averaged over the last year (24) of Lagrangian simulations with NEMOWAVE currents, for (c,e) the global ocean, (d,f) the Pacific, (i,k) the Atlantic and (j,l) the Indian Ocean. Each section is decomposed into a zoom on the first 100 m (c,d,i,j) and then on the rest of the section, thus for 100–5000 m left (e,f,k,l). For each ocean basin, the surface plastic concentration is plotted as a function of latitude for the NEMOWAVE model (black) and the NEMOREF model (gray): Global (a), Pacific (b), Atlantic (g) and Indian (h) ocean.

combining the concentrations calculated in each basin (Fig. 4). 5.24 % of the total amount of plastic released during the simulation remains between 0 and 1 m depth at the end of the 24-year coupled simulation (Table 1). This fraction accounts for 8.2 million tons of plastic in this layer. In contrast, nearly half of this number (3.8 million tons) is stuck at the sea surface for the ocean experiment NEMOREF. The most striking differences are thus seen close to the sea surface for all ocean basins, particularly in the Pacific Ocean where the plastic concentration is eight times greater with the coupled experiment (Fig. 4). The differences between the coupled and uncoupled experiments (normal line and dashed black line, respectively) on the total amount of microplastics versus depth are explained mainly by the concentration changes in the North Pacific Ocean between 0 and 400 m depth Fig. 4b. Plastic concentration is the highest in the Pacific Ocean at the sea surface and below 10 m depth, yet entering the ocean, the concentrations in the Indian Ocean are the highest, relative to their volume, for the two experiments (Fig. 4a). Nevertheless, particle concentration of the Indian Ocean as a function of depth does not differ significantly for the two simulations, NEMOREF and NEMOWAVE, and its surface concentration is about 0.07–0.1 g m^{-3} on average. Below 400 m, the differences are small for all ocean basins and it's not shown in Fig. 4a. Another notable feature is the negative bias for tropical where NEMOREF centralizes more plastic (Fig. 4b). The difference between NEMOWAVE and NEMOREF surface plastic concentration also highlights the retention of plastic by the coupled experiment for 1° the subtropical gyres and higher latitudes, 2° the Mediterranean Sea and the Sea of Japan (Fig. 4b).

The ocean layer located under the thermocline, delimited by depths >1000 m (Table 1), concentrates the lowest amount of plastic (1.4 % and 1.84 %) since, after 24 years of advection, just a few quantities could reach these depths. Nevertheless, uncertainties arise for longer simulations that will release more plastic into the ocean. Fig. 4 does not show these depths, as this effect was already identified in the previous Fig. 3, and the concentrations were too small to be visible on the same graph. Furthermore, the two regions of the water column between 100 m and 1000 m concentrate most of the plastic, where nearly 60 % of the total amount remains at the end of the simulation (Table 1) with 87.7 and 84.0 million tons of plastic for the uncoupled and coupled experiment, respectively. The fraction of plastic in the uppermost layers for the coupled model is mostly lost and compensated for in the latter depth range. Furthermore, the amount of plastic in the water column between 1 and 100 m does not differ between experiments, with 7.34 % (7.40 %) for the 1–10 m range and 32.60 % (31.68 %) for the 10–100 m range for the uncoupled (respectively coupled) simulation.

3.3. Vertical velocity fields

We now investigate the modeled vertical velocities which are the cause of the large differences in the amount of particles found in the surface layer.

Fig. 5 shows the zonally averaged vertical velocities at 1 and 10 m depth, time-averaged over 2014–2017 for the NEMOWAVE and NEMOREF model simulations. The most visible differences between the velocities of the coupled and uncoupled simulations are observed for mid and high latitudes beyond 30°. For latitudes between 30° and 50–55°, the vertical velocities below the surface layer are upward for NEMOWAVE, especially in the Southern Hemisphere, which will tend to retain plastic particles at the sea surface, whereas vertical velocities in NEMOREF are downward. The largest differences are found at the Southern Ocean latitudes where the largest waves are found, with maximum zonally averaged values up to 10^{-7} m s^{-1} around 45°S. Half of these amplitudes are found in the Northern Hemisphere. In contrast, negative differences are found in the equatorial region from 10°S to 10°N, and south of 60°S. To understand these differences, we have computed the vertical velocities induced by the divergence of the horizontal Stokes transport (Fig. 5, green) and it clearly explains the difference between the two models near the sea surface. In the same way wind-induced Ekman transports induce vertical Ekman pumping below the Ekman layer, the wave-induced Stokes transports in the upper layers induce horizontal divergence that must be compensated by vertical velocities from below. Some differences with the well-know Ekman processes are that the surface layer influenced by Stokes drift is thinner than the Ekman layer, and that the regions of convergence and divergence are not exactly the same. Stokes transport roughly follows the wind direction, even remotely, whereas Ekman transport is orthogonal to the wind because of the Coriolis force. Hence the global trades/westerlies wind pattern forcing the waves induces upward'Stokes pumping' vertical velocities poleward of 30° latitude, and downward vertical velocities below the surface in the equatorial region. It is well known that the Stokes transport is associated with the so-called Stokes-Coriolis force, which essentially generates a return transport compensating the Stokes transport (Hasselmann, 1970). The Ekman pumping below the Ekman layer is therefore not affected by the Stokes transport (McWilliams and Restrepo, 1999). Nonetheless, this compensation occurs in a depth-averaged sense. Close to the surface, Stokes drift divergence can be significant and influence the vertical displacement of plastic particles.

The full geographical pattern of these vertical velocities shows a

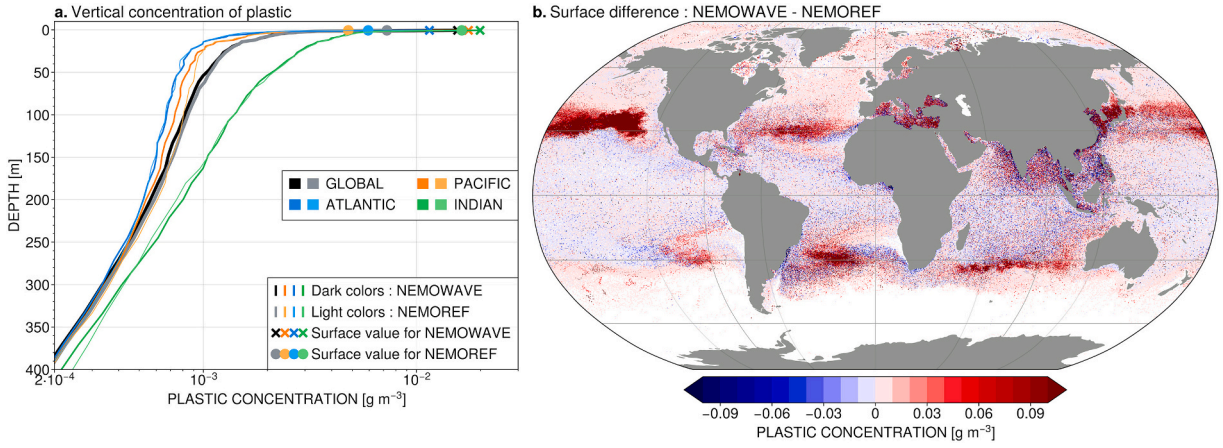

Fig. 4. (a) Horizontally averaged plastic concentration as a function of depth (g m^{-3}) for each ocean basin at the end of the 24-year Lagrangian simulations with the NEMOREF (light colors) and NEMOWAVE (dark colors) currents. Only the upper 400 m are shown. Each ocean basin is depicted by a specific color: gray, orange, blue and green accounts for respectively the Global, Pacific, Atlantic and Indian Ocean. Note the logarithmic scale used for plastic concentration. (b) Difference in surface concentration between the two simulations NEMOWAVE-NEMOREF (red for positive difference, blue for negative). (For interpretation of the references to color in this figure legend, the reader is referred to the web version of this article.)

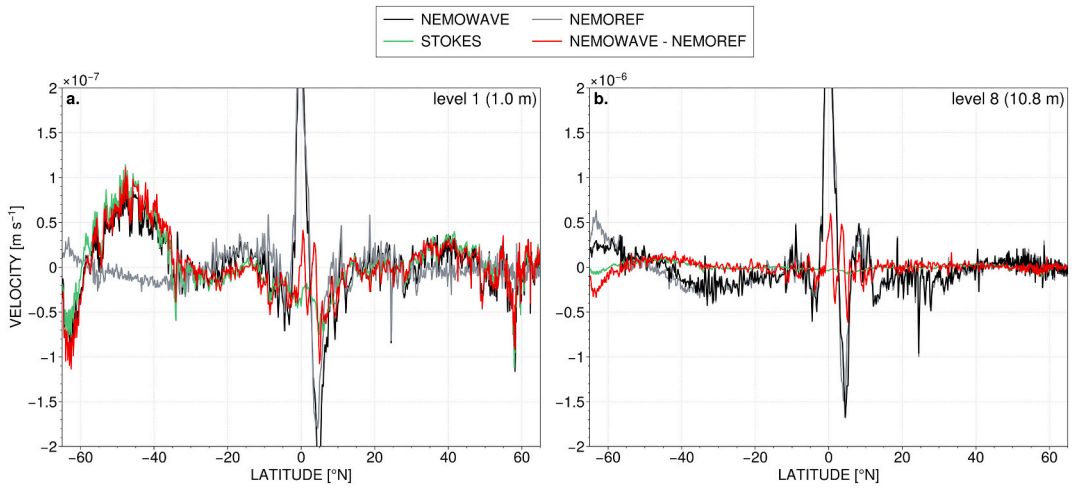

Fig. 5. Zonally averaged vertical velocities at (a) 1 m and (b) 10.8 m depths, time-averaged over the whole period 2014–2017 for the NEMOWAVE (black) and NEMOREF (gray) models (m s^{-1}), for the difference between NEMOWAVE and NEMOREF (red), and for the vertical velocities computed from the horizontal divergence of the Stokes transport provided by the WW3 wave model to the NEMOWAVE ocean model (green). Note the change in scale for the velocities between (a) and (b). (For interpretation of the references to color in this figure legend, the reader is referred to the web version of this article.)

more complex structure with a strong zonal asymmetry between western and eastern boundaries (Fig. 6). The difference between the NEMOWAVE coupled experiment and the NEMOREF reference experiment is mainly positive except in the equatorial region and at high latitudes (Fig. 6d). Negative differences are also present near coastal regions and below 60°S where Stokes drift convergence induces downward vertical velocity in the coupled experiment when averaged over the whole period. At 1 m depth, the predominant signal remains the strong upward vertical velocities at mid-latitudes poleward of 30° in the coupled model. These velocities contribute to the retention of plastic particles at the surface on their way to the center of convergence zones, but surprisingly, the time-averaged vertical velocities at the latitude of maximum plastic concentration (30°) are close to zero for both models. The difference between NEMOWAVE and NEMOREF vertical velocities

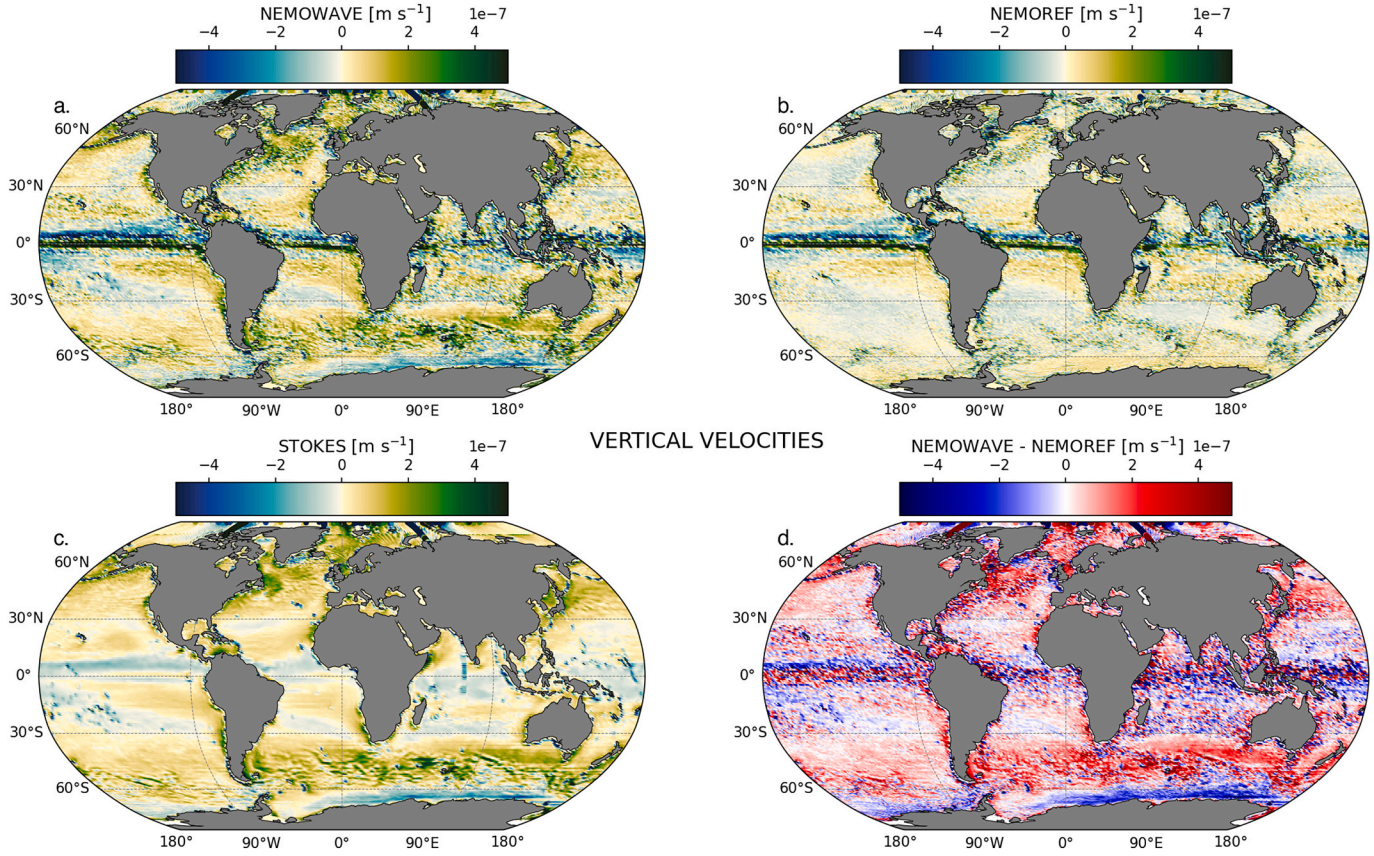

Fig. 6. Vertical velocities at 1 m depth averaged over the whole period 2014–2017 for the NEMOWAVE (a) and NEMOREF (b) models (m s^{-1}), and difference between the NEMOWAVE and NEMOREF models (d). Vertical velocities computed from the horizontal divergence of the Stokes transport provided by the WW3 wave model to the NEMOWAVE ocean model (c).

has the same patterns and amplitude as the ones computed from the divergence of horizontal Stokes velocities (Fig. 6c,d). The Southern Hemisphere shows the highest upward Stokes velocities in the Roaring Forties and Furious Fifties. High waves are evidenced in the same area, at all times of the year by Couvelard et al. (2020, their Fig. 3). These upward velocities are not observed with the same amplitude in the Northern Hemisphere except above the North Atlantic western boundary currents, off Newfoundland and the Labrador Sea. Hence, within the subtropical gyres, the vertical velocities induced by Stokes drift are slightly positive, especially in the Atlantic, Indian and East Pacific basins.

4. Discussion

The realistic discharge scenario highlights the importance of waves in the three-dimensional drift of plastic in the oceans. Plastic release from coasts and rivers, modeled after Lebreton et al. (2017) and Lebreton and Andrady (2019), allows us to represent the state of oceanic plastic pollution including >80 % of the plastic at sea (Jambeck et al., 2015). Our results are consistent with the current understanding of plastic at sea, at least for the surface layers (Cózar et al., 2014). Particles are concentrated at the surface in the subtropical gyres where their concentration is very high. The structure of the surface convergence zones is also similar to what has been previously obtained using two-dimensional (Chenillat et al., 2021; Dobler et al., 2019) or three-dimensional (Huck et al., 2022) currents calculated by ocean simulations using the NEMO code.

The realistic discharge experiments show that neutral microplastic particles primarily enter the deep ocean through the Ekman current convergence zones around 30° latitude, and that these neutral particles discharged from land can reach these convergence zones with the majority of their trajectories at the surface. Thus, the particles flow mainly toward the convergence zones following geostrophic and Ekman currents before diving to depth. A significant portion of the surface and deep concentrations of microplastics are also found near discharge locations.

Our results are in agreement with available observations of deep ocean plastic (Egger et al., 2020; Pabortsava and Lampitt, 2020; Ross et al., 2021; Vega-Moreno et al., 2021; Zhao et al., 2022) and complement the previous conclusions of other studies (Huck et al., 2022) that the water column is a reservoir of neutral plastic, now with the inclusion of the influence of waves and a fully coupled wave-ocean experiment. A strong dispersion of neutral plastic particles is notable around two to three hundred meters depth with both simulations (coupled and uncoupled), similar to what has been noted in previous ocean observations by Pabortsava and Lampitt (2020) and in a simulation with an uncoupled ocean model by Huck et al. (2022). Therefore, there will be a strong presence of neutral particles at the surface in the subtropical gyres, but also at depth where the particles will disperse and spread over large latitude bands. This dispersion is slightly stronger for the coupled model and extends over about forty degrees of latitude below each surface convergence zone for both experiments. We also find the importance of vertical dynamics, especially in the North Pacific Subtropical Gyre, with a significant subsurface plunge of the particles (Egger et al., 2020).

Coupling the global ocean model and currents with waves, as done by Couvelard et al. (2020), is a step forward in evaluating the convergence and areas of high plastic concentration. Strong differences were found in the first layers of the ocean, where Stokes drift has a major impact. The amount of plastic in the uppermost model layer was multiplied by more than two (exactly 2.14 for the land-based scenario) using the model fully coupled with waves. Our results indicate that waves may increase the retention of neutral plastic particles at the surface because of the upward vertical velocities induced by the divergence of Stokes transport in the surface layers. Therefore, taking into account the effect of waves on the fate of plastic particles in the ocean is necessary to understand the tropical patterns of concentrations and partially answer the main question: where is all the plastic (van Sebille et al., 2020)? Consideration of Stokes drift could also be useful for ocean plastic collection missions, which may require appropriate locations. Indeed, plastic-concentrated surface regions had different shapes in the coupled and uncoupled experiments.

Moreover, a large number of plastic particles were studied with both simulations (over 16 million for all river and coastal land-based emission scenarios), providing a sufficiently large number of trajectories to study precisely the different pathways that plastics would likely take from their release. Plastics remain mainly in oceanic basins close to their release, with the example of the North Pacific, but they can also accumulate for some time between islands and in quasi-enclosed basins.

The actual resolution at a quarter of degree allows accuracy on the convergence zones and does not differ from one of the latest studies with an already higher resolution at 1/12° (Huck et al., 2022). These conclusions direct our future work toward a proper consideration of the influence of waves on current at higher spatial resolution and near the coast. Upcoming work to implement current-wave coupling at higher space and time resolution will also support and discuss these first results on the importance of wave coupling in particle retention, and thus for the retention of plastic near the coast and in semi-enclosed basins such as the Mediterranean and the Sea of Japan.

The issue of beaching, of which waves and swell may act as a significant driver (Dobler et al., 2022), was not addressed in this study because, in the three-dimensional framework, the use of non-divergent currents in the Lagrangian model does not allow for the trapping of particles along the coast. Beaching in two-dimensional surface Lagrangian experiments depends strongly on the horizontal divergence of nearshore currents (Chenillat et al., 2021), and this divergent component is particularly sensitive to the addition of Stokes drift (Dobler et al., 2019) and windage (Chassignet et al., 2021). Taking beaching into consideration in our simulations should be implemented by a specific parametrization in the coastal grid cells (Jalón-Rojas et al., 2019; Baudena et al., 2022; Dobler et al., 2022), but the calibration and robust validation of such a parametrization would require a data-set of cross-validated observational data that is not yet available at the global scale. Another issue is the horizontal resolution of the global model ∂(10 km), which may not be the appropriate scale to address the coastline details, bathymetric and topographic, that influence beaching (Haarr et al., 2019). Moreover, experimental studies performed by Forsberg et al. (2020) demonstrate that beaching of marine litter may be influenced by complex interactions of wind, waves, currents and litter physical properties (density, size, shape). Therefore, many parameters should be considered, all with sufficient resolution, in order to simulate plastic beaching appropriately. In this context, our 3D and global approach should be viewed as a step in the constitution of appropriate boundary conditions for regional models better able to consider and quantify plastic beaching on specific regions.

However, only neutral plastics were tracked in our simulation based on estimations of mismanaged plastic waste from coastal populations and river inputs. Physically speaking, this represents just a fraction (neutral plastic accounts for 19 % of the discharges (Mountford and Morales Maqueda, 2021)) of what actually enters the sea which includes both buoyant and non-buoyant particles. Non-buoyant plastic accounts for approximately 40 % of the global plastic production (Andrady, 2011), which is one of the primary sources of plastic. Some work can be conducted by adding different particle velocities in simulations, especially on the vertical, as already explored by sea ice particles (Mountford and Morales Maqueda, 2019, 2021) in an Eulerian framework. The simulations studied in this paper were carried out with 'neutral' particles in order to directly measure the influence of waves on plastic distribution. Future work will involve the different floatabilities of plastic particles to provide an improved account of the current state of the ocean. A second step to consider is the interaction with marine biology, which is poorly constrained to date (Lobelle et al., 2021), but may have a

first-order impact on three-dimensional marine plastic transport.

CRediT authorship contribution statement

Raphaël Bajon: Data curation, Visualization, Investigation, Writing – Original draft preparation. **Thierry Huck**: Methodology, Supervision, Conceptualization, Writing - Reviewing and Editing. **Nicolas Grima**: Conceptualization, Ariane Software support, Writing - Reviewing and Editing. **Christophe Maes**: Conceptualization, Writing - Reviewing and Editing. **Bruno Blanke**: Conceptualization, Ariane Software, Writing - Reviewing and Editing. **Camille Richon**: Conceptualization, Writing - Reviewing and Editing. **Xavier Couvelard**: Software (ocean-wave coupled model development and simulations), Writing - Reviewing and Editing.

Declaration of competing interest

The authors declare that they have no known competing financial interests or personal relationships that could have appeared to influence the work reported in this paper.

Data availability

The original plastic particle release scenario components are available on figshare for river (Lebreton et al., 2017) and coastal population (Lebreton and Andrady, 2019). Coupled and uncoupled velocity fields are available on request. Our annual average plastic concentration after 24 years of advection by both models (needed to assess the conclusion of the paper) can be downloaded from the plastic folder on Github (https://github.com/RaphaelBajon/plastic-progress).

Acknowledgements

The authors are grateful for the support of the ISblue grant, Interdisciplinary graduate school for the blue planet (ANR-17-474 EUREOOI5), which made this work possible. The authors would also like to thank Sébastien Hervé, who helped draw Fig. 1, Alison Chalm for proofreading the English and Nicolas Rascle for his comments on the wave coupling. The NEMO-WW3 ocean-wave coupled model was developed in the framework of the ALBATROS project funded by CMEMS (MERCATOR-Océan).

References

Andrady, A.L., 2011. Microplastics in the marine environment. Mar. Pollut. Bull. 62, 1596–1605. https://doi.org/10.1016/j.marpolbul.2011.05.030.

Arakawa, A., Lamb, V.R., 1977. Computational design of the basic dynamical processes of the ucla general circulation model. URL:. In: Chang, J. (Ed.), General Circulation Models of the Atmosphere, volume 17 of Methods in Computational Physics: Advances in Research and Applications. Elsevier, pp. 173–265. https://doi.org/10.1016/B978-0-12-460817-7.50009-4 https://www.sciencedirect.com/science/article/pii/B9780124608177500094.

Barnier, B., Madec, G., Penduff, T., Molines, J.M., Treguier, A.M., Sommer, J.L., Beckmann, A., Biastoch, A., Böning, C., Dengg, J., Derval, C., Durand, E., Gulev, S., Remy, E., Talandier, C., Theetten, S., Maltrud, M., McClean, J., Cuevas, B.D., 2006. Impact of partial steps and momentum advection schemes in a global circulation model at eddy permitting resolution. Ocean Dyn. 56, 543–567. https://doi.org/10.1007/s10236-006-0082-1.

Baudena, A., Ser-Giacomi, E., Jalón-Rojas, I., Galgani, F., Pedrotti, M.L., 2022. The streaming of plastic in the Mediterranean Sea. Nat. Commun. 13, 2981. https://doi.org/10.1038/s41467-022-30572-5.

Blackwatters, J., Holmes, D., Carr, L., 2020. A geography of marine plastics. Ir. Geogr. 53, 59–92. https://doi.org/10.2014/igj.v53i1.1411.

Blanke, B., Raynaud, S., 1997. Kinematics of the Pacific equatorial undercurrent: an eulerian and lagrangian approach from GCM results. J. Phys. Oceanogr. 27, 1038–1053. https://doi.org/10.1175/1520-0485(1997)027<1038:KOTPEU>2.0.CO;2.

Blanke, B., Speich, S., Madec, G., Maugé, R., 2002. A global diagnostic of interior ocean ventilation. Geophys. Res. Let. 29, 1–4. https://doi.org/10.1029/2001GL013727.

Borrelle, S., Ringma, J., Lavender Law, K., Monnahan, C., Lebreton, L., McGivern, A., Murphy, E., Jambeck, J., Leonard, G., Hilleary, M., Eriksen, M., Possingham, H., De Frond, H., Gerber, L., Polidoro, B., Tahir, A., Bernard, M., Mallos, N., Barnes, M., Rochman, C., 2020. Predicted growth in plastic waste exceeds efforts to mitigate plastic pollution. Science 369, 1515–1518. https://doi.org/10.1126/science.aba3656.

Breivik, O., Mogensen, K., Bidlot, J.R., Balmaseda, M.A., Janssen, P.A.E.M., 2015. Surface wave effects in the NEMO Ocean model: forced and coupled experiments. J. Geophys. Res. Oceans 120, 2973–2992. https://doi.org/10.1002/2014JC010565.

Chassignet, E., Xu, X., Zavala-Romero, O., 2021. Tracking marine litter with a global ocean model: where does it go? Where does it come from? Front. Mar. Sci. 8, 667591 https://doi.org/10.3389/fmars.2021.667591.

Chenillat, F., Huck, T., Maes, C., Grima, N., Blanke, B., 2021. Fate of floating plastic debris released along the coasts in a global ocean model. Mar. Pollut. Bull. 165, 112116 https://doi.org/10.1016/j.marpolbul.2021.112116.

Couvelard, X., Lemarié, F., Samson, G., Redelsperger, J.L., Ardhuin, F., Benshila, R., Madec, G., 2020. Development of a 2-way coupled ocean-wave model: assessment on a global NEMO(v3.6)-WW3(v6.02) coupled configuration. Geosci. Model Dev. 13, 3067–3090. https://doi.org/10.5194/gmd-13-3067-2020.

Cózar, A., Echevarría, F., González-Gordillo, J.I., Irigoien, X., Úbeda, B., Hernández-León, S., Palma, Á.T., Navarro, S., García-de Lomas, J., Ruiz, A., Fernández-de Puelles, M.L., Duarte, C.M., 2014. Plastic debris in the open ocean. Proc. Natl. Acad. Sci. 111, 10239–10244. https://doi.org/10.1073/pnas.1314705111.

Dobler, D., Huck, T., Maes, C., Grima, N., Blanke, B., Martinez, E., Ardhuin, F., 2019. Large impact of stokes drift on the fate of surface floating debris in the south Indian Basin. Mar. Pollut. Bull. 148, 202–209. https://doi.org/10.1016/j.marpolbul.2019.07.057.

Dobler, D., Maes, C., Martinez, E., Rahmania, R., Gautama, B.G., Farhan, A.R., Dounias, E., 2022. On the fate of floating marine debris carried to the sea through the main rivers of Indonesia. URL: J. Mar. Sci. Eng. 10, 1009. https://doi.org/10.3390/jmse10081009 https://www.mdpi.com/2077-1312/10/8/1009.

Egger, M., Sulu-Gambari, F., Lebreton, L., 2020. First evidence of plastic fallout from the North Pacific garbage patch. Sci. Rep. 10, 7495. https://doi.org/10.1038/s41598-020-64465-8.

Eriksen, M., Lebreton, L.C.M., Carson, H.S., Thiel, M., Moore, C.J., 2014. Plastic pollution in the world's oceans: more than 5 trillion plastic pieces weighing over 250,000 tons afloat at sea. PLoS ONE 9, e111913. https://doi.org/10.1371/journal.pone.0111913.

Forsberg, P.L., Sous, D., Stocchino, A., Chemin, R., 2020. Behaviour of plastic litter in nearshore waters: first insights from wind and wave laboratory experiments. Mar. Pollut. Bull. 153, 111023 https://doi.org/10.1016/j.marpolbul.2020.111023.

Galgani, F., Brien, A.S., Weis, J., 2021. Are litter, plastic and microplastic quantities increasing in the ocean? Microplastics Nanoplastics 1, 2. https://doi.org/10.1186/s43591-020-00002-8.

van Gennip, S.J., Dewitte, B., Garçon, V., 2019. In search for the sources of plastic marine litter that contaminates the Easter Island ecoregion. Sci. Rep. 9 https://doi.org/10.1038/s41598-019-56012-x.

GESAMP, 2015. Sources, Fate and Effects of Microplastics in the Marine Environment: A Global Assessment. Technical Report 90. IMO/FAO/UNESCO-IOC/UNIDO/WMO/IAEA/UN/UNEP/UNDP Joint Group of Experts on the Scientific Aspects of Marine Environmental Protection, Rep. Stud. GESAMP.

Geyer, R., Lambeck, J., Law, K.L., 2017. Production, use, and fate of all plastics ever made. Sci. Adv. 3, e1700782 https://doi.org/10.1126/sciadv.1700782.

Haarr, M.L., Westerveld, L., Fabres, J., Iversen, K.R., Busch, K.E.T., 2019. A novel GIS-based tool for predicting coastal litter accumulation and optimising coastal cleanup actions. Mar. Pollut. Bull. 139, 117–126. https://doi.org/10.1016/j.marpolbul.2018.12.025.

Hasselmann, K., 1970. Wave-driven inertial oscillations. Geophys. Fluid Dyn. 1, 463–502. https://doi.org/10.1080/03091927009365783.

Huang, R., 2015. Oceanographic topics | surface/wind driven circulation. URL:. In: North, G.R., Pyle, J., Zhang, F. (Eds.), Encyclopedia of Atmospheric Sciences (Second Edition), second edition. Academic Press, Oxford, pp. 301–314. https://doi.org/10.1016/B978-0-12-382225-3.00280-2 https://www.sciencedirect.com/science/article/pii/B9780123822253002802.

Huck, T., Bajon, R., Grima, N., Portela, E., Molines, J.M., Penduff, T., 2022. Three-dimensional dispersion of neutral "plastic" particles in a global ocean model. Front. Anal. Sci. 2, 868515 https://doi.org/10.3389/frans.2022.868515.

Isobe, A., Azuma, T., Cordova, M., Cózar, A., Galgani, F., Hagita, R., 2021. A multilevel dataset of microplastic abundance in the world's upper ocean and the laurentian great lakes. Microplastics Nanoplastics 1. https://doi.org/10.1186/s43591-021-00013-z.

Jalón-Rojas, I., Wang, X.H., Fredj, E., 2019. A 3D numerical model to track marine plastic debris (TrackMPD): sensitivity of microplastic trajectories and fates to particle dynamical properties and physical processes. Mar. Pollut. Bull. 141, 256–272. https://doi.org/10.1016/j.marpolbul.2019.02.052.

Jambeck, J.R., Geyer, R., Wilcox, C., Siegler, T.R., Perryman, M., Andrady, A., Narayan, R., Law, K.L., 2015. Plastic waste inputs from land into the ocean. Science 347, 768–771. https://doi.org/10.1126/science.1260352.

Kooi, M., van Nes, E.H., Scheffer, M., Koelmans, A.A., 2017. Ups and downs in the ocean: effects of biofouling on vertical transport of microplastics. Environ. Sci. Technol. 51, 7963–7971. https://doi.org/10.1021/acs.est.6b04702.

Kubota, M., 1994. A mechanism for the accumulation of floating marine debris north of Hawaii. J. Phys. Oceanogr. 24, 1059–1064. https://doi.org/10.1175/1520-0485.

Kukulka, T., Proskurowski, G., Morét-Ferguson, S., Meyer, D.W., Law, K.L., 2012. The effect of wind mixing on the vertical distribution of buoyant plastic debris. Geophys. Res. Let. 39 https://doi.org/10.1029/2012GL051116.

Lau, W.W.Y., Shiran, Y., Bailey, R.M., Cook, E., Stuchtey, M.R., Koskella, J., Velis, C.A., Godfrey, L., Boucher, J., Murphy, M.B., Thompson, R.C., Jankowska, E., Castillo, A.C., Pilditch, T.D., Dixon, B., Koerselman, L., Kosior, E., Favoino, E., Gutberlet, J.,

Baulch, S., Atreya, M.E., Fischer, D., He, K.K., Petit, M.M., Sumaila, U.R., Neil, E., Bernhofen, M.V., Lawrence, K., Palardy, J.E., 2020. Evaluating scenarios toward zero plastic pollution. Science 369, 1455–1461. https://doi.org/10.1126/science.aba9475.

Law, K.L., 2017. Plastics in the marine environment. Annu. Rev. Mar. Sci. 9, 205–229. https://doi.org/10.1146/annurev-marine-010816-060409.

Lebreton, L., Andrady, A., 2019. Future scenarios of global plastic waste generation and disposal. Palgrave Commun. 5 https://doi.org/10.1057/s41599-018-0212-7.

Lebreton, L., Greer, S.D., Borrero, J.C., 2012. Numerical modelling of floating debris in the world's oceans. Mar. Pollut. Bull. 64, 653–661. https://doi.org/10.1016/j.marpolbul.2011.10.027.

Lebreton, L., van der Zwet, J., Damsteeg, J.W., Slat, B., Andrady, A., Reisser, J., 2017. River plastic emissions to the world's oceans. Nat. Commun. 8 https://doi.org/10.1038/ncomms15611.

Lobelle, D., Kooi, M., Koelmans, A.A., Laufkötter, C., Jongedijk, C.E., Kehl, C., van Sebille, E., 2021. Global modeled sinking characteristics of biofouled microplastic. J. Geophys. Res. Oceans. https://doi.org/10.1029/2020JC017098.

Madec, G., 2012. NEMO ocean general circulation model reference manual. Technical Report 27. In: Note du Pôle de modélisation, Institut Pierre-Simon Laplace (IPSL), Paris, France.

Maes, C., Grima, N., Blanke, B., Martinez, E., Paviet-Salomon, T., Huck, T., 2018. A surface, "Superconvergence" pathway connecting the South Indian Ocean to the subtropical South Pacific gyre. Geophys. Res. Let. 45, 1915–1922. https://doi.org/10.1002/2017GL076366.

Maes, T., Perry, J., Alliji, K., Clarke, C., Birchenough, S.N., 2019. Shades of grey: marine litter research developments in Europe. URL: Mar. Pollut. Bull. 146, 274–281. https://doi.org/10.1016/j.marpolbul.2019.06.019 https://www.sciencedirect.com/science/article/pii/S0025326X19304655.

Martinez, E., Maamaatuaiahutapu, K., Taillandier, V., 2009. Floating marine debris surface drift: convergence and accumulation toward the South Pacific subtropical gyre. Mar. Pollut. Bull. 58, 1347–1355.

Maximenko, N., Hafner, J., Niiler, P., 2012. Pathways of marine debris derived from trajectories of lagrangian drifters. Mar. Pollut. Bull. 65, 51–62. https://doi.org/10.1016/j.marpolbul.2011.04.016.

McWilliams, J.C., Restrepo, J.M., 1999. The wave-driven ocean circulation. J. Phys. Oceanogr. 29, 2523–2540. https://doi.org/10.1175/1520-0485(1999)029<2523:TWDOC>2.0.CO;2.

van der Mheen, M., Pattiaratchi, C., van Sebille, E., 2019. Role of Indian ocean dynamics on accumulation of buoyant debris. J. Geophys. Res. Oceans 124, 2571–2590. https://doi.org/10.1029/2018JC014806.

Mountford, A.S., Morales Maqueda, M.A., 2019. Eulerian modelling of the three-dimensional distribution of seven popular microplastic types in the global ocean. J. Geophys. Res. Oceans 124, 8558–8573. https://doi.org/10.1029/2019JC015050.

Mountford, A.S., Morales Maqueda, M.A., 2021. Modeling the accumulation and transport of microplastics by sea ice. J. Geophys. Res. Oceans 126, e2020JC016826. https://doi.org/10.1029/2020JC016826.

Onink, V., van Sebille, E., Laufkötter, C., 2022. Empirical lagrangian parametrization for wind-driven mixing of buoyant particles at the ocean surface. Geosci. Model Dev. 15, 1995–2012. https://doi.org/10.5194/gmd-15-1995-2022.

Onink, V., Wichmann, D., Delandmeter, P., van Sebille, E., 2019. The role of Ekman currents, geostrophy and stokes drift in the accumulation of floating microplastics. J. Geophys. Res. Oceans 124. https://doi.org/10.1029/2018JC014547.

Pabortsava, K., Lampitt, R.S., 2020. High concentrations of plastic hidden beneath the surface of the Atlantic Ocean. Nat. Commun. 11, 4073. https://doi.org/10.1038/s41467-020-17932-9.

Pattiaratchi, C., van der Mheen, M., Schlundt, C., Narayanaswamy, B.E., Sura, A., Hajbane, S., White, R., Kumar, N., Fernandes, M., Wijeratne, S., 2022. Plastics in the Indian Ocean – sources, fate, distribution and impacts. Ocean Sci. 18, 1–28. https://doi.org/10.5194/os-18-1-2022.

Plastics Europe, 2019. Plastics – the Facts 2019. An analysis of European plastics production, demand and waste data. Technical Report. URL:. Plastics Europe Association of Plastics Manufacturers https://plasticseurope.org/knowledge-hub/plastics-the-facts-2019/.

Reisser, J., Slat, B., Noble, K., du Plessis, K., Epp, M., Proietti, M., de Sonneville, J., Becker, T., Pattiaratchi, C., 2015. The vertical distribution of buoyant plastics at sea: an observational study in the North Atlantic gyre. Biogeosciences 12, 1249–1256. https://doi.org/10.5194/bg-12-1249-2015.

Ross, P., Chastain, S., Vassilenko, E., Etemadifar, A., 2021. Pervasive distribution of polyester fibres in the Arctic Ocean is driven by Atlantic inputs. Nat. Commun. 12, 106. https://doi.org/10.1038/s41467-020-20347-1.

Schmidt, C., Krauth, T., Wagner, S., 2017. Export of plastic debris by rivers into the sea. Environ. Sci. Technol. 51, 12246–12253. https://doi.org/10.1021/acs.est.7b02368.

van Sebille, E., Aliani, S., Law, K.L., Maximenko, N., Alsina, J., Bagaev, A., Bergmann, M., Chapron, B., Chubarenko, I., Cózar, A., Delandmeter, P., Egger, M., Fox-Kemper, B., Garaba, S.P., Goddijn-Murphy, L., Hardesty, D., Hoffman, M.J., Isobe, A., Jongedijk, C., Kaandorp, M., Khatmullina, L., Koelmans, A.A., Kukulka, T., Laufkötter, C., Lebreton, L., Lobelle, D., Maes, C., Martinez-Vicente, V., Maqueda, M. A.M., Poulain-Zarcos, M., Rodriguez, E., Ryan, P.G., Shanks, A., Shim, W.J., Suaria, G., Thiel, M., van den Bremer, T., Wichmann, D., 2020. The physical oceanography of the transport of floating marine debris. Environ. Res. Lett. 15, 023003 https://doi.org/10.1088/1748-9326/ab6d7d.

van Sebille, E., England, M.H., Froyland, G., 2012. Origin, dynamics and evolution of ocean garbage patches from observed surface drifters. Environ. Res. Lett. 7, 044040. http://stacks.iop.org/1748-9326/7/i=4/a=044040.

van Sebille, E., Wilcox, C., Lebreton, L., Maximenko, N., Hardesty, B.D., van Franeker, J. A., Eriksen, M., Siegel, D., Galgani, F., Law, K.L., 2015. A global inventory of small floating plastic debris. Environ. Res. Lett. 10, 124006 https://doi.org/10.1088/1748-9326/10/12/124006.

Speich, S., Blanke, B., Cai, W., 2007. Atlantic meridional overturning circulation and the southern hemisphere supergyre. Geophys. Res. Let. 34, L23614 https://doi.org/10.1029/2007GL031583.

Speich, S., Lutjeharms, J.R.E., Penven, P., Blanke, B., 2006. Role of bathymetry in agulhas current configuration and behaviour. Geophys. Res. Let. 33, L23611 https://doi.org/10.1029/2006GL027157.

Tekman, M.B., Wekerle, C., Lorenz, C., Primpke, S., Hasemann, C., Gerdts, G., Bergmann, M., 2020. Tying up loose ends of microplastic pollution in the Arctic: distribution from the sea surface, through the water column to deep-sea sediments at the HAUSGARTEN observatory. Environ. Sci. Technol. 54, 4079–4090. https://doi.org/10.1021/acs.est.9b06981.

Vega-Moreno, D., Abaroa-Pérez, B., Rein-Loring, P.D., Presas-Navarro, C., 2021. Distribution and transport of Microplastics in the upper 1150 m of the water column at the Eastern North Atlantic Subtropical Gyre, Canary Island, Spain. Sci. Total Environ. 788 https://doi.org/10.1016/j.scitotenv.2021.147802.

WAVEWATCH III® Development Group, 2016. User Manual and System Documentation of WAVEWATCH III ® Version 5.16, Tech. Note 329. Technical Report. NOAA/NWS/NCEP/MMAB, College Park, MD, USA.

Weiss, L., Ludwig, W., Heussner, S., Canals, M., Ghiglione, J.F., Estournel, C., Constant, M., Kerhervé, P., 2021. The missing ocean plastic sink: gone with the rivers. Science 373, 107–111. https://doi.org/10.1126/science.abe0290.

Woodall, L.C., Sanchez-Vidal, A., Canals, M., Paterson, G.L.J., Coppock, R., Sleight, V., Calafat, A., Rogers, A.D., Narayanaswamy, B.E., Thompson, R.C., 2014. The deep sea is a major sink for microplastic debris. R. Soc. Open Sci. 1, 140317 https://doi.org/10.1098/rsos.140317.

Wright, S.L., Thompson, R.C., Galloway, T.S., 2013. The physical impacts of microplastics on marine organisms: a review. Environ. Pollut. 178, 483–492. https://doi.org/10.1016/j.envpol.2013.02.031.

Zhao, S., Zettler, E.R., Bos, R.P., Lin, P., Amaral-Zettler, L.A., Mincer, T.J., 2022. Large quantities of small microplastics permeate the surface ocean to abyssal depths in the South Atlantic gyre. Glob. Chang. Biol. 28, 2991–3006. https://doi.org/10.1111/gcb.16089.